Eur. Phys. J. C (2011) 71: 1510
DOI 10.1140/epjc/s10052-010-1510-4

THE EUROPEAN PHYSICAL JOURNAL C

Letter

Percolation of color sources and the equation of state of QGP in central Au–Au collisions at $\sqrt{s_{NN}} = 200$ GeV

R.P. Scharenberg, B.K. Srivastava[a], A.S. Hirsch

Department of Physics, Purdue University, West Lafayette, IN 47907, USA

Received: 10 August 2010 / Revised: 29 September 2010 / Published online: 20 January 2011

Abstract The Color String Percolation Model (CSPM) is used to determine the equation of state (EOS) of the Quark–Gluon Plasma (QGP) produced in central Au–Au collisions at $\sqrt{s_{NN}} = 200$ A GeV using STAR data at RHIC. When the initial density of interacting colored strings exceeds the 2D percolation threshold a cluster is formed, which defines the onset of color deconfinement. These interactions also produce fluctuations in the string tension which transforms the Schwinger particle (gluon) production mechanism into a maximum entropy thermal distribution analogous to QCD Hawking–Unruh radiation. The single string tension is determined by identifying the known value of the universal hadron limiting temperature $T_c = 167.7 \pm 2.6$ MeV with the CSPM temperature at the critical percolation threshold parameter $\xi_c = 1.2$. At midrapidity the initial Bjorken energy density and the initial temperature determine the number of degrees of freedom consistent with the formation of a $\sim 2+1$ flavor QGP. An analytic expression for the equation of state, the sound velocity $C_s^2(\xi)$ is obtained in CSPM. The CSPM $C_s^2(\xi)$ and the bulk thermodynamic values energy density ε/T^4 and entropy density s/T^3 are in excellent agreement in the phase transition region with recent lattice QCD simulations (LQCD) by the HotQCD Collaboration.

All high energy soft multihadron interactions exhibit thermal patterns of abundances characterized by the same temperature, independent of the center of mass energy [1]. The hadron limiting temperatures were measured by statistical thermal analyses that fit the data with a minimum of parameters [1]. In heavy-ion collisions it may be plausible that multiple parton interactions produce a thermalized system. In (p, p), $(p, \bar{p})$ and (p, A) collisions multiple parton interactions are not likely to thermalize the system. In (e^+e^-) annihilation where thermal behavior is observed, the multiparton mechanism may also be an inappropriate explanation [2–4].

The determination of the EOS of hot, strongly interacting matter is one of the main challenges of strong interaction physics (HotQCD Collaboration) [5]. Recent LQCD calculations for the bulk thermodynamic observables, e.g. pressure, energy density, entropy density and for the sound velocity have been reported [5]. In the present work a percolation model coupled with hydrodynamics has been utilized to calculate these quantities and compare them with the LQCD results.

The CSPM describes the initial collision of two heavy ions in terms of color strings stretched between the projectile and target. Color strings may be viewed as small discs in the transverse space filled with the color field created by colliding partons. With growing energy and size of the colliding nuclei the number of strings grows and start to overlap to form clusters [6, 7]. The interactions of strings reduces the hadron multiplicity μ and increases the average transverse momentum $\langle p_T^2 \rangle$ of these hadrons, so that the total transverse momentum is conserved. The observables μ, and $\langle p_t^2 \rangle$ are directly related to the field strength in the string and thus to the generating color. For a cluster of n strings

$$n = \frac{\mu}{\mu_0} \frac{\langle p_t^2 \rangle}{\langle p_t^2 \rangle_1}, \tag{1}$$

where μ_0 is the multiplicity of hadrons from a single string and $\langle p_t^2 \rangle_1$ is the average transverse momentum squared of a single string. The CSPM model calculation for hadron multiplicities and momentum spectra was found to be in excellent agreement with experiment [8, 9]. Within the framework of clustering of color sources, the elliptic flow, v_2, and the dependence of the nuclear modification factor on the azimuthal angle show reasonable agreement with the RHIC data [10]. The critical density of percolation is related to the effective critical temperature and thus percolation may

[a] e-mail: brijesh@purdue.edu

be the way to achieve deconfinement in the heavy-ion collisions [11]. An additional important check of this interacting string approach was provided by the measurement of Long Range forward–backward multiplicity Correlations (LRC) by the STAR group at RHIC [12, 13].

2D percolation is a non-thermal second order phase transition, but in CSPM the Schwinger barrier penetration mechanism for particle production and the fluctuations in the associated string tension due to the strong string interactions make it possible to define a temperature. Consequently the particle spectrum is "born" with a thermal distribution [11, 14]. The percolation threshold at which the spanning cluster appear, a "connected" system of color sources, identifies the percolation phase transition.

Above the percolation threshold this system is considered to be in the deconfined phase, which subsequently expands according to Bjorken boost invariant 1D hydrodynamics [15].

With an increasing number of strings n there is a progression from isolated individual strings to clusters and then to a large cluster which suddenly spans the area. In two dimensional percolation theory the relevant quantity is the dimensionless percolation density parameter given by [6, 7]

$$\xi = \frac{N S_1}{S_N}, \tag{2}$$

where N is the number of strings formed in the collisions and S_1 is the transverse area of the a single string and S_N is the transverse nuclear overlap area. The critical cluster which spans S_N, appears for $\xi_c \geq 1.2$ [16]. As ξ increases the fraction of S_N covered by this spanning cluster increases.

The color suppression factor $F(\xi)$, reduces the hadron multiplicity from $n\mu_0$ to the interacting string value μ

$$\mu = F(\xi) n \mu_0, \tag{3}$$

$$F(\xi) = \sqrt{\frac{1 - e^{-\xi}}{\xi}}. \tag{4}$$

To evaluate the initial value of ξ from data, a parameterization of p–p events at 200 GeV is used to compute the p_t distribution [17]

$$dN_c/dp_t^2 = a/(p_0 + p_t)^{\alpha}, \tag{5}$$

where a, p_0, and α are parameters used to fit the data. This parameterization also can be used for nucleus–nucleus collisions to take into account the interactions of the strings [17]

$$p_0 \to p_0 \left(\frac{\langle n S_1/S_n \rangle_{Au-Au}}{\langle n S_1/S_n \rangle_{pp}} \right)^{1/4}, \tag{6}$$

where S_n corresponds to the area occupied by the n overlapping strings. The thermodynamic limit, i.e. letting n and $S_n \to \infty$ while keeping ξ fixed, is used to evaluate

$$\left\langle \frac{n S_1}{S_n} \right\rangle = 1/F^2(\xi), \tag{7}$$

$$dN_c/dp_t^2 = \frac{a}{(p_0 \sqrt{F(\xi_{pp})/F(\xi)} + p_t)^{\alpha}}. \tag{8}$$

In pp collisions $\langle n S_1/S_n \rangle_{pp} \sim 1$ due to the low string overlap probability. The factor $1 - e^{-\xi}$ in (4) corresponds to the fractional area covered by the spanning cluster. The STAR analysis of charged hadrons for 0–10% central Au + Au collisions at $\sqrt{s_{NN}} = 200$ GeV gives a value $\xi = 2.88 \pm 0.09$ [17].

The strong longitudinal chromo-electric fields produce Schwinger–Bialas [11, 14, 18] like radiation with a thermal spectrum, in analogy with the Hawking–Unruh radiation [19–24]. Both the Schwinger–Bialas and Hawking–Unruh derivations lead to the same value of the maximum entropy temperature. Above the critical value of ξ, the QGP in CSPM consists of massless constituents (gluons). The percolation parameter ξ determines the cluster size distribution, the temperature $T(\xi)$ and the transverse momentum in the collision [11]. The connection between ξ and the temperature $T(\xi)$ involves the Schwinger mechanism (SM) for particle production. In CSPM the Schwinger distribution for massless particles is expressed in terms of p_t^2

$$dn/dp_t^2 \sim e^{-\pi p_t^2/x^2} \tag{9}$$

with the average value of string tension, $\langle x^2 \rangle$. Gaussian fluctuations in the string tension (Bialas) around its mean value transforms SM into the thermal distribution [14]

$$dn/dp_t^2 \sim e^{\left(-p_t \sqrt{\frac{2\pi}{\langle x^2 \rangle}}\right)} \tag{10}$$

with $\langle x^2 \rangle = \pi \langle p_t^2 \rangle_1 / F(\xi)$. The temperature is given by

$$T(\xi) = \sqrt{\frac{\langle p_t^2 \rangle_1}{2F(\xi)}}. \tag{11}$$

The string percolation density parameter ξ which characterizes the percolation clusters also determines the temperature of the system. In this way at $\xi_c = 1.2$ the percolation phase transition at $T(\xi_c)$ models the thermal deconfinement transition. In the determination of temperature using (11) the value of $F(\xi)$ is obtained using the experimental data [17]. We will adopt the point of view that the experimentally determined chemical freeze-out temperature is a good measure of the phase transition temperature, T_c [25]. The single string average transverse momentum $\langle p_t^2 \rangle_1$ is calculated at $\xi_c = 1.2$ with the universal chemical freeze-out temperature of 167.7 ± 2.6 MeV [1]. This gives $\sqrt{\langle p_t^2 \rangle_1} = 207.2 \pm 3.3$ MeV which is close to $\simeq$200 MeV

used previously in the calculation of the percolation transition temperature [11]. Above $\xi_c = 1.2$ the size and density of the spanning cluster increases. We use the measured value of $\xi = 2.88$ to determine the temperature, before the expansion, $T_i = 193.6 \pm 3.0$ MeV of the quark–gluon plasma in reasonable agreement with $T_i = 221 \pm 19^{\text{stat}} \pm 19^{\text{sys}}$ from the enhanced direct photon experiment measured by the PHENIX Collaboration [26].

The QGP according to CSPM is born in local thermal equilibrium because the temperature is determined at the string level. We use CSPM coupled to hydrodynamics to calculate energy density, pressure, entropy density and sound velocity. As mentioned earlier, the strings interact strongly to form clusters and produce the pressure at the early stages of the collisions, which is evident from the presence of elliptical flow in CSPM [10]. After the initial temperature $T > T_c$ the CSPM perfect fluid may expand according to Bjorken boost invariant 1D hydrodynamics [15]:

$$\frac{1}{T}\frac{dT}{d\tau} = -C_s^2/\tau, \tag{12}$$

$$\frac{dT}{d\tau} = \frac{dT}{d\varepsilon}\frac{d\varepsilon}{d\tau}, \tag{13}$$

$$\frac{d\varepsilon}{d\tau} = -Ts/\tau, \tag{14}$$

$$s = \left(1 + C_s^2\right)\frac{\varepsilon}{T}, \tag{15}$$

$$\frac{dT}{d\varepsilon}s = C_s^2, \tag{16}$$

where ε is the energy density, s the entropy density, τ the proper time, and C_s the sound velocity.

Above the critical temperature only massless particles are present in CSPM. The initial energy density ε_i above T_c is given by [15]

$$\varepsilon_i = \frac{3}{2}\frac{\frac{dN_c}{dy}\langle m_t\rangle}{S_n \tau_{\text{pro}}}. \tag{17}$$

To evaluate ε_i we use the charged pion multiplicity dN_c/dy at midrapidity and S_n values from STAR for 0–10% central Au–Au collisions with $\sqrt{s_{NN}} = 200$ GeV [27]. The factor 3/2 in (17) accounts for the neutral pions. We can calculate $\langle p_t\rangle$ using the CSPM thermal distribution (10) and (11). For $0.2 < p_t < 1.5$, $\langle p_t\rangle = 0.394 \pm 0.003$ GeV, adding the extra energy required for the rest mass of pions at hadronization $\langle m_t\rangle = 0.42 \pm 0.003$ GeV. The error on $\langle p_t\rangle$ is due to the error on T_i.

The dynamics of massless particle production has been studied in QE2 quantum electrodynamics. QE2 can be scaled from electrodynamics to quantum chromodynamics using the ratio of the coupling constants [28]. The production time τ_{pro} for a boson (gluon) is [29]

$$\tau_{\text{pro}} = \frac{2.405\hbar}{\langle m_t\rangle}. \tag{18}$$

Using (17) and (18) gives $\varepsilon_i = 2.27 \pm 0.16$ GeV/fm^3 at $\xi = 2.88$. In CSPM the total transverse energy is proportional to ξ. From the measured value of ξ and ε it is found that ε is proportional to ξ for the range $1.2 < \xi < 2.88$, $\varepsilon_i = 0.788\ \xi$ GeV/fm^3 [17, 27]. This relationship has been extrapolated to below $\xi = 1.2$ and above $\xi = 2.88$ for the energy and entropy density calculations. The Au–Au at $\sqrt{s_{NN}} = 200$ GeV data are used to normalize the CSPM ε/T^4 values. Figure 1 shows ε/T^4 as obtained from CSPM along with the LQCD calculations [5] and the CSPM pressure $3p/T^4$.

The number of degrees of freedom (DOF) is related to the energy density,

$$\varepsilon_i = \frac{G(T)\pi^2 T_i^4}{30(\hbar c)^3}. \tag{19}$$

At T_i the DOF is 37.5 ± 3.6. At T_c, $\varepsilon_c = 0.95 \pm 0.07$ GeV/fm^3 and 27.7 ± 2.6 DOF.

The sound velocity requires the evaluation of s and $dT/d\varepsilon$, which can be expressed in terms of ξ and $F(\xi)$. With $q^{1/2} = F(\xi)$ one obtains

$$\frac{dT}{d\varepsilon} = \frac{dT}{dq}\frac{dq}{d\xi}\frac{d\xi}{d\varepsilon}. \tag{20}$$

Then C_s^2 becomes

$$C_s^2 = \left(1 + C_s^2\right)(-0.25)\left(\frac{\xi e^{-\xi}}{1 - e^{-\xi}} - 1\right) \tag{21}$$

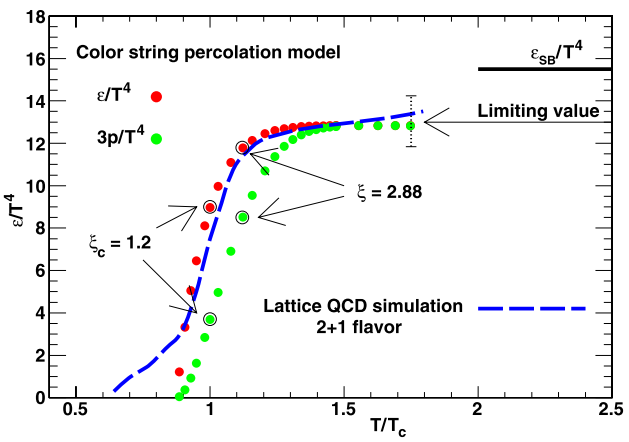

Fig. 1 The energy density from CSPM versus T/T_c^{CSPM} (*red circles*) and Lattice QCD energy density vs. T/T_c^{LQCD} (*blue dash line*) for $2+1$ flavor and p4 action [5]. $3p/T^4$ is also shown for CSPM with *green circles*

for $\xi \geq \xi_c$, an analytic function of ξ for the equation of state of the QGP for $T \geq T_c$.

Figure 2 shows the comparison of C_s^2 from CSPM and LQCD. The LQCD values were obtained using the EOS of $2+1$ flavor QCD at finite temperature with physical strange quark mass and almost physical light quark masses [5]. At $T/T_c = 1$ the CSPM and LQCD agree with the C_s^2 value of the physical hadron gas with resonance mass truncation $M \leq 2.5$ GeV [30].

The entropy density s/T^3 is computed using (15) as shown in Fig. 3 along with the LQCD results. CSPM is in excellent agreement with the LQCD calculations in the phase transition region for $T/T_c \leq 1.5$. It is noteworthy that CSPM at $\xi > \xi_c$ exhibits gluon saturation effects similar to the Color Glass Condensate (CGC) [31]. The saturation scale Q_s in CGC corresponds to $\langle p_t^2 \rangle_1 / F(\xi)$ in CSPM. It has been pointed out that the most challenging task for coupling the CGC to a hydrodynamic expansion is the question of thermalization [32, 33].

In summary, the present analysis consists of using the ξ values from data, identifying the universal chemical temperature with the critical percolation density parameter ξ_c, establishing the direct proportionality between ε_i and ξ and using the functional dependence of $T(\xi)$ and ε_i to obtain C_s^2. Thus we can determine the temperature dependence of energy density, pressure and entropy density in the color string percolation picture. The results are also in agreement with lattice QCD in the phase transition region, when the results are plotted with respect to T/T_c^{CSPM} and T/T_c^{LQCD}. The value of $C_s^2 = 0.14$ is in agreement with the physical resonance gas value at the critical temperature. The non-interacting high temperature limit for $C_s^2 = 0.33$ is reached at $T \sim 1.5 T_c$.

The percolation critical transition is known to represent a continuous phase transition. In central Au–Au collisions at

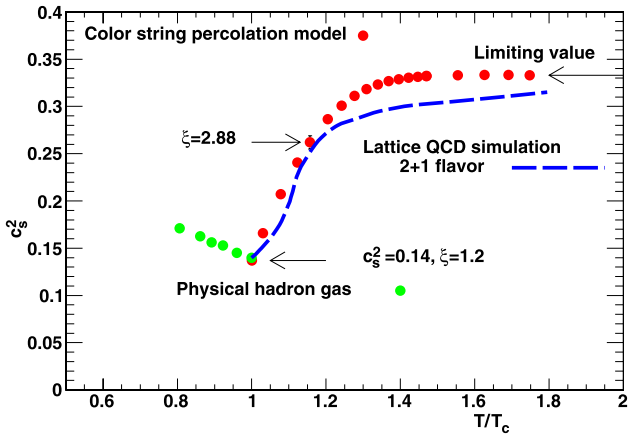

Fig. 2 The speed of sound from CSPM versus T/T_c^{CSPM} (*red circles*) and Lattice QCD-p4 speed of sound versus T/T_c^{LQCD} (*blue dash line*)[5]. The physical hadron gas with resonance mass cut off $M \leq 2.5$ GeV is shown as *solid green circles* [30]

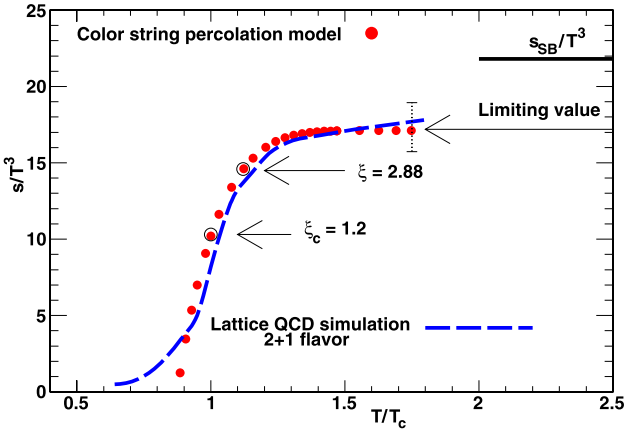

Fig. 3 The entropy density from CSPM versus T/T_c^{CSPM} (*red circle*) and Lattice QCD entropy density vs. T/T_c^{LQCD} (*blue dash line*) [5]

$\sqrt{s_{NN}} = 200$ GeV the QCD to hadron phase transition for baryon density $\mu_B \sim 0$ is believed to be a cross-over transition which does not have a latent heat [34]. The CSPM EOS correctly describes the QCD to hadron cross-over transition and provides an answer to the question of the origin of the universal temperature observed in A–A, p–p and e^+e^- collisions.

The percolation analysis of the color sources applied to STAR data at RHIC provides a compelling argument that the QGP is formed in central Au–Au collisions at $\sqrt{s_{NN}} =$ 200 GeV. It also suggests that the QGP is produced in all soft high energy high multiplicity collisions when the string density exceeds the percolation transition. A further definitive test of CSPM can be made at LHC energies by comparing hadron–hadron and nucleus–nucleus collisions.

Acknowledgements We express our thanks to C. Pajares and N. Armesto for many fruitful discussions. This research was supported by the Office of Nuclear Physics within the U.S. Department of Energy Office of Science under Grant No. DE-FG02-88ER40412.

References

1. F. Becattini, P. Castorina, A. Milov, H. Satz, Eur. Phys. J. C **66**, 377 (2010)
2. F. Becattini, P. Castorina, J. Manninen, H. Satz, Eur. Phys. J. C **56**, 493 (2008)
3. H. Satz, Eur. Phys. J. Spec. Top. **155**, 167 (2008)
4. A. Andronic et al., Phys. Lett. B **675**, 312 (2009)
5. A. Bazavov et al., Phys. Rev. D **80**, 014504 (2009)
6. M.A. Braun, C. Pajares, Eur. Phys. J. C **16**, 349 (2000)
7. M.A. Braun, F. del Moral, C. Pajares, Phys. Rev. C **65**, 024907 (2002)
8. J. Dias de Deus, E.G. Ferreiro, C. Pajares, R. Ugoccioni, Eur. Phys. J. C **40**, 229 (2005)

9. P. Brogueira, J. Dias de Deus, J.G. Milhano, Nucl. Phys. A **832**, 76 (2010)
10. I. Bautista, L. Cunqueiro, J. Dias de Deus, C. Pajares, J. Phys. G **37**, 015103 (2010)
11. J. Dias de Deus, C. Pajares, Phys. Lett. B **642**, 455 (2006)
12. P. Brogueira, J. Dias de Deus, J.G. Milhano, Phys. Rev. C **76**, 064901 (2007)
13. B.I. Abelev et al. (STAR Collaboration), Phys. Rev. Lett. **103**, 172301 (2009)
14. A. Bialas, Phys. Lett. B **466**, 301 (1999)
15. J.D. Bjorken, Phys. Rev. D **27**, 140 (1983)
16. H. Satz, Rep. Prog. Phys. **63**, 1511 (2000)
17. B.K. Srivastava, R.P. Scharenberg, T. Tarnowsky (STAR Collaboration), Nukleonika **51**, s109 (2006)
18. J. Schwinger, Phys. Rev. **82**, 664 (1951)
19. S.W. Hawking, Commun. Math. Phys. **43**, 199 (1975)
20. W.G. Unruh, Phys. Rev. D **14**, 870 (1976)
21. M.K. Parikh, F. Wilczek, Phys. Rev. Lett. **85**, 5042 (2000)
22. D. Kharzeev, K. Tuchin, Nucl. Phys. A **753**, 316 (2005)
23. D. Kharzeev, E. Levin, K. Tuchin, Phys. Rev. C **75**, 044903 (2007)
24. P. Castorina, D. Kharzeev, H. Satz, Eur. Phys. J. C **52**, 187 (2007)
25. P. Braun-Munzinger, J. Stachel, C. Wetterich, Phys. Lett. B **596**, 61 (2004)
26. A. Adare et al. (PHENIX Collaboration), Phys. Rev. Lett. **104**, 132301 (2010)
27. B.I. Abelev et al. (STAR Collaboration), Phys. Rev. C **79**, 34909 (2009)
28. C.Y. Wong, *Introduction to High Energy Heavy Ion Collisions* (World Scientific, Singapore, 1994)
29. J. Schwinger, Phys. Rev. **128**, 2425 (1962)
30. P. Castorina, J. Cleymans, D.E. Miller, H. Satz, arXiv:0906.2289v1 [hep-ph]
31. J. Schaffner-Bielich, D. Kharzeev, L. McLerran, R. Venugopalan, Nucl. Phys. A **705**, 494 (2002)
32. F. Gelis, Nucl. Phys. (2010). doi:10.1016/j.nuclphysa.2010.09.001
33. K. Dusling, T. Epelbaum, F. Gelis, R. Venugopalan, arXiv:1009.4363v1 [hep-ph]
34. Z. Fodor, PoSLATT2007:011 (2007)